Assessment of the Fire Resistance Test With Respect to Beams in Real Structures

SUSAN LAMONT, BARBARA LANE, ASIF USMANI and DOUGAL DRYSDALE

Historically fire resistance design of structures has been based upon single element behavior in the standard fire resistance test. Engineers have always recognized that whole frame structural behavior in fire cannot be described by a test on a single element. However, it is only in relatively recent years since the Broadgate phase 8 fire (SCI, 1991) and the subsequent Cardington frame fire tests that researchers have fully investigated and understood the behavior of whole structures in response to fire. The University of Edinburgh in collaboration with Imperial College and Corus (formally British Steel) have played a major role in this field of research through the UK Department of Environment and Transport in the Regions (DETR), Partners in Technology (PiT) project. Significant progress towards a complete understanding of the structural behavior of highly redundant composite steel frames in fire has been achieved (Edinburgh University, 2000).

Single element behavior in the fire resistance test is a gross simplification of the true behavior of structural elements as part of a whole building in real fire conditions. No account is taken of the interactions between the structural elements in the region of the fire and the rest of the cooler surrounding structure. In a statically determinate structure, such as a solitary simply-supported beam, there is only one load path determined by equilibrium considerations alone. An indeterminate structure such as a multi-story frame is capable of transferring load through many alternate load paths. Consequently the pattern of forces and stresses in an indeterminate beam are determined by the relative stiffness of other members of the structure based on both equilibrium and compatibility considerations. If a structure has adequate ductility and stability the redundancy under fire conditions enables the structure to find different load paths and mechanisms to continue supporting additional load when its strength has been reached at a single location.

Susan Lamont is fire engineer, Arup Fire, Ove Arup and Partners, London, UK.

Barbara Lane is senior fire engineer, Arup Fire, Ove Arup and Partners, London, UK.

Asif Usmani is senior lecturer, School of Engineering and Electronics, University of Edinburgh, UK.

Dougal Drysdale is professor, School of Engineering and Electronics, University of Edinburgh, UK.

Elements of construction tested in the fire resistance furnace have to meet some or all of three criteria. These include their ability to maintain load-bearing capacity, integrity, and insulation. In this discussion we are concerned with the failure of a beam in terms of its load-bearing capacity. BS 476 Part 20 (BSI, 1987) states that the failure of a load-bearing horizontal element will have occurred when either a deflection of $l/20$ is achieved or the rate of deflection (mm/min) calculated over 1 minute intervals exceeds the limit described by Equation 1. However this limit should only be applied beyond a deflection of $l/30$

$$\text{Rate of deflection} = \frac{l^2}{9000d} \quad (1)$$

where

l = clear span of the specimen, mm

d = the distance from the top of the structural section to the bottom of the design tension zone, mm

Material degradation under constant loading at high temperatures is the reason for high deflections or "runaway" in axially unrestrained, simply-supported beams tested in the fire resistance test. Consequently, our understanding of the failure of structures at high temperatures has centered on understanding material degradation. Indeed loading and material degradation have long been considered as the key factors in determining the fire resistance of structures. Modelling and investigation of the Cardington frame fire tests (Edinburgh University, 2000 and Usmani, Rotter, Lamont, Sanad, and Gille, 2001) has shown that thermal expansion and thermal bowing of structural elements as a result of the heating regime dominate the response of the structure. Material degradation and loading are secondary issues, which only become important near impending "runaway" which in most cases is never reached in "real" fires.

The large deflections experienced in the composite slab of the Cardington frame of which Figure 1 is an example and in the Broadgate Phase 8 building (SCI, 1991) are to a large extent a direct result of thermal expansion and thermal bowing effects. The deflections are associated predominantly with thermal strains, not mechanical strains, and as such are not detrimental to the structure. This is discussed in more detail by Usmani et al. (2001) and later in this paper.

If large displacements are not detrimental for the structure and therefore an unreliable indicator of structural distress, failure must be defined in a different manner. The way forward for structural fire safety design is to consider the structure as a whole and to explicitly state what the intent of the design really is, i.e. life safety or property protection. Performance-based design of structures in fire traditionally addresses whole building structures in terms of compartment fire behavior (for example time-equivalent methods, natural fires). However this level of sophistication is not easily carried through to the structural behavior as a result of such fires. It is this that needs to be addressed in order to achieve the safe and efficient design of structures for fire.

HISTORY OF THE FIRE RESISTANCE TEST

It can be said that fire resistance test methods relate to the behavior of components and structures in the post-flashover stage of a fully developed fire. The methods enable elements of construction such as walls, floors, columns and beams to be assessed according to their ability to remain stable, resist the passage of flame and hot gases and provide resistance to heat transmission.

Fire resistance testing of construction was formalized about 80 years ago although testing had been going on prior to that in an unplanned and informal manner (Malhotra, 1980). The main reason for testing was that insurance companies needed to have some comparative evaluation between different types of construction. The earliest recorded tests in the United Kingdom were on a floor by the associated architects in the 1790s, on a column in Munich by the technical high school in 1884 and on a floor in the USA by the Denver Equitable Building in 1890. The main test station in the UK at Borehamwood was opened in 1935.

Early tests were carried out in brick huts using wood as a fuel where the floor or wall under test was part of the hut itself. Early testing was very simple. Construction was tested and observations made of its behavior, primarily with reference to collapse and to the transfer of fire to the unexposed side of the wall or floor. An international fire prevention congress was held in 1910 with the aim of getting agreement on an international temperature-time history for fire tests. However, it was not until 1918 that a standard temperature-time curve was accepted. The first ASTM standard C19 (now E119) (ASTM, 1995) was published in 1918 (Malhotra, 1980). The first British Standard to describe the temperature-time curve was not published until 1932. Equation 2 describes the temperature-time history for the British Standard tests (BS 476 Part 20 (BSI, 1987)).

$$T = T_0 + 345\log(0.133t + 1) \qquad (2)$$

where

t = time, sec

T = temperature of the furnace atmosphere next to the specimen, °C

The ASTM temperature-time curve is described by a series of points. The curves are very similar as shown in Figure 2. However, differences in heating regimes occur in furnaces around the world. The heating regime is dependent on the construction of the furnace; particularly the thermal inertia of the wall linings. Construction shape influences the degree of turbulence and thus convective heat transfer. However, more importantly the thermal inertia of the wall linings affect the radiative heat transfer to the element under testing.

The standard temperature-time curve bears little resemblance to a real fire temperature-time history. It has no growth or decay phase and as such does not represent any real fire although it is designed to typify temperatures experienced during the post-flashover phase of most fires (Malhotra, 1980). Figure 3 illustrates the temperature-time histories of "real" fires, of varying fire load and ventilation, together with the standard curve. Ingberg (1928) was the first to propose a solution to this problem when he suggested that fire severity could be related to the fire load of a room and expressed as an area under the temperature-time curve. The severity of two fires were equal if the area under the temperature-time curves were equal (above a base line of 300°C). Thus any fire temperature-time history could be associated to the standard curve. This approach was based on limited information from room fire tests.

Most regulatory bodies accepted Ingberg's fire severity approach and fire resistance testing to the standard temperature-time curve continued. The requirements for fire resistance were related to the assumed levels of fire loads in different occupancies. This approach was highly inappro-

Fig. 1. Deflected shape of the Cardington frame after the "BS Corner Test."

priate because it took no account of the factors which dictate the severity of a compartment fire namely, ventilation, compartment dimensions and the properties of the boundary wall linings (Drysdale, 1998).

EQUIVALENT FIRE EXPOSURE

Since Ingberg's early attempt at relating the severity of the standard fire to a real compartment fire, many researchers have developed similar but more sophisticated relationships. The time equivalent concept makes use of the fire load and ventilation data in a real compartment fire to produce a value, which would be "equivalent" to the exposure time in the standard test. Law (1971) defines t-equivalence as the exposure time in the standard fire resistance test which gives the same heating effect on a structure as a given compartment fire. Formulating equivalent fire exposures has traditionally been achieved by gathering data from room-burn experiments where steel temperatures were recorded and variables relating to the fire severity were systematically changed (e.g. ventilation, fire load, compartment shape).

Law (1971) developed a time equivalence relationship to include the effect of ventilation using data gathered from a CIB study of fully developed compartment fires (Thomas and Heselden, 1972). This relationship is described by Equation 3. Pettersson, Magnusson, and Thor (1976), adopted Law's method of t-equivalence and developed the expression using the family of calculated temperature-time curves for particular compartments derived by Magnusson and Thelanderson (1970). Pettersson's t-equivalence approach takes into consideration the effect of the thermal inertia of the compartment wall lining (see Equation 4). The normalized heat load concept is one of the most recent developments in this area and was introduced by Harmathy (1987) although it has not been readily adopted. The normalized heat load is defined as the heat absorbed by the element per unit surface area during fire exposure.

Law's T-equivalence formula

$$\tau_e = 0.022 \frac{A_F L}{\sqrt{\left[A_v (A_t - A_F - A_v)\right]}} \tag{3}$$

Pettersson's T-equivalence formula

$$\tau_e = 0.31 C \frac{A_F L}{(A_t A_v \sqrt{h_v})^{\frac{1}{2}}} \tag{4}$$

where

τ_e = Equivalent fire resistance, h
A_F = floor area, m^2
A_t = total area of the compartment boundaries including the compartment opening, m^2
A_v = Area of the ventilation opening, m^2
L = Fire load, kg/m^2
C = factor depending on the thermal absorptivity of the compartment boundaries, $hm^{3/4}kg^{-1}$
h_v = height of ventilation opening, m

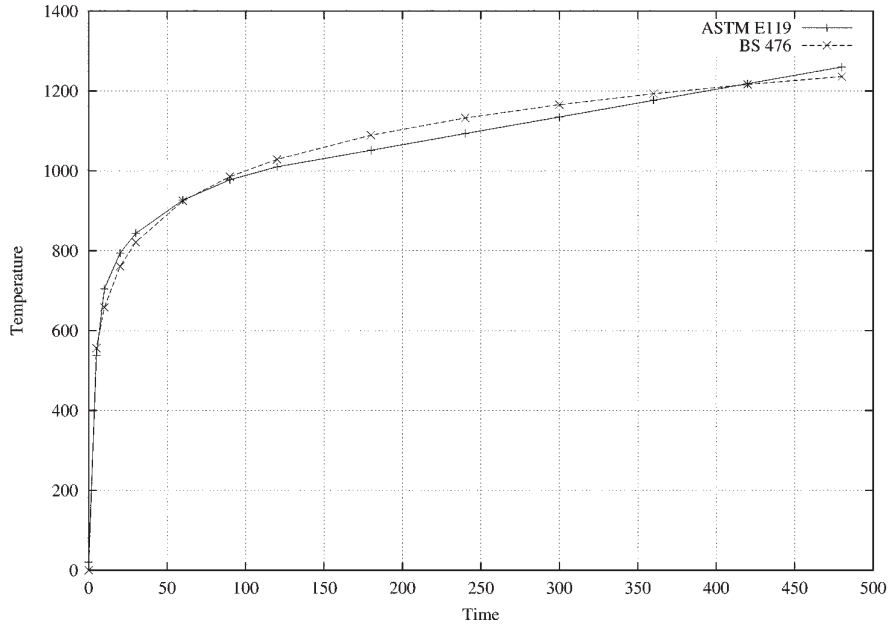

Fig. 2. Standard temperature-time curves.

NATURAL FIRE METHOD

With the t-equivalence approach the heating effect in a compartment is calculated based on real compartment fire behavior and that heating is related back to the standard furnace test. In more recent times however, the energy and mass balance equations for the fire compartment are used to model the thermal exposure and fire duration. This is known as the natural fire method. In this method the combustion characteristics of the fire load, the ventilation effects and the thermal properties of the compartment enclosure are considered. This is not related in anyway to the standard fire resistance test and provides an estimate of the real fire duration, once flashover has occurred.

The standard fire curve, t-equivalence and natural fire curves can all be used to determine the behavior of structures in fire. The natural fire method is clearly the most realistic means of determining fire exposure.

CURRENT METHODS OF FIRE RESISTANCE TESTING

Techniques for conducting fire tests have not changed significantly in the last 60 years. Fire resistance testing consists of subjecting a prototype sample of the construction to prescribed heating conditions in a furnace and judging its performance based on specified criteria. The fire resistance test as it is in the United Kingdom is described by BS 476: Parts 20-23 (BSI, 1987) *Fire tests on building materials and structures.* Part 21 details the methods for the determination of the fire resistance of load bearing elements. During the British standard tests on load bearing elements the support conditions provided during the test can be similar to that which would apply in service. However, when the service conditions are unknown the test beam or slab is installed as simply-supported, i.e. axially unrestrained to thermal expansion. A similar test exists in the US (ASTM, 1995) where restrained and unrestrained assemblies have different conditions of acceptance based on particular temperature criteria. Although testing in the US recognizes the benefits of indeterminate structures through providing end restraint, test conditions are still removed from integrated behavior found in real buildings. Although the test provides restraint to expansion, contraction is not supported, which in real structures helps develop the vital secondary load carrying mechanism of tensile membrane action.

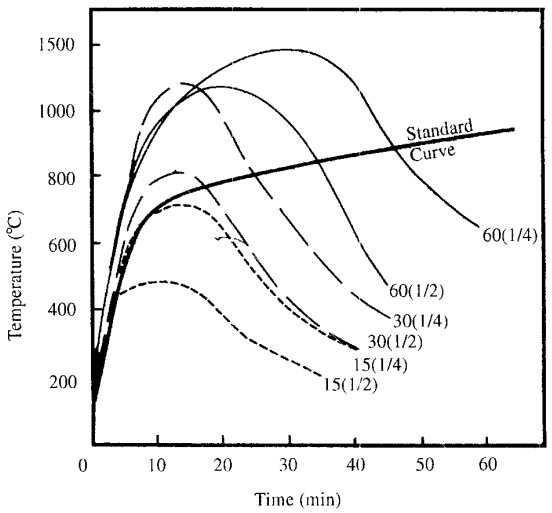

Fig. 3. Comparison of the standard fire curve and real fire temperature-time histories. The fire load is in kg/m² and the ventilation opening (shown in parenthesis) is a fraction of one wall (Drysdale, 1998).

METHODS OF CALCULATING FIRE PROTECTION THICKNESS

The level of fire resistance for a particular building is related to the fire load available and the size or height of the building. If the temperature of the steel structure will exceed 550°C in a period of time less than the fire resistance specified by Approved Document B then the fire protection thickness is prescribed using the "yellow book" (ASFP, 2000) or calculated using BS5950 Part 8 (BSI, 1990) or EC3 Part 1.2 or EC4 Part 1.2.

The "yellow book" approach uses fire test data in accordance with BS 476 Part 21 (BSI, 1987). All approved fire protection materials have been tested in accordance with BS 476 and the required thickness of each product has been evaluated with regard to fire resistance period and section factor. These results are all based on a limiting steel temperature of 550°C.

BS 5950 Part 8 (BSI, 1990) allows a slightly more sophisticated approach. The engineer calculates the load ratio of the beam (Equation 5).

$$\text{Load Ratio} = \frac{\text{Applied moment at the fire limit state}}{\text{Moment capacity at } 20\,^{\circ}\text{C}} = \frac{M_f}{M_C} \qquad (5)$$

If the load ratio is low (i.e. the moment capacity at 20°C is high compared to the applied moment at the fire limit state), roughly less than 0.7, then the upper limit of the steel temperature may be greater than 550°C. Methods described in EC3 Part1.2 or EC4 Part 1.2 are very similar.

NEW UNDERSTANDING

As a direct result of the PiT project, sponsored by the DETR(UK) and undertaken by Edinburgh University in collaboration with British Steel (now CORUS) and Imperial College, a greater understanding of the behavior of steel-framed structures in fire has been realized. The project involved modelling the four British Steel compartment fire tests carried out on the BRE Cardington 8-story composite steel frame. The output from the models produced a wealth

of information about structural behavior in real fires that needed to be rigorously understood. The key message as a result of this understanding is that composite-framed structures of the type tested at Cardington possess reserves of strength through adopting large displacement configurations. Thermally induced forces and displacements dominate pre-failure behavior rather than material degradation and loading as previously assumed (Usmani et al., 2001). In order to understand the behavior of structural elements exposed to fire the most fundamental relationships are described by the following equation (creep strains, although very important for some materials, are not entirely relevant to the current discussion and hence do not appear in the equation):

$$\varepsilon_{total} = \varepsilon_{thermal} + \varepsilon_{mechanical} \quad (6)$$

where

$\varepsilon_{mechanical} \Rightarrow \sigma$ (stresses)
$\varepsilon_{total} \Rightarrow \delta$ (deflections)

The total strains govern the deflected shape of the structure but the mechanical strains alone govern the stress state in the structure. The effect of fire is manifested as thermal expansion and thermal bowing in structural elements. Usmani et al. (2001) describes in detail the effects of thermal expansion and thermal bowing on structural elements. Only a very brief description will be given in the next section.

THERMAL EXPANSION AND THERMAL BOWING

Figures 4 and 5 respectively illustrate the effects of thermal expansion and thermal bowing independently on a simple beam. If the beam is axially free it will expand with no mechanical straining in response to a uniform mean temperature rise. Thermal bowing will result in a uniform curvature ($\phi=\alpha T_{,y}$) where $T_{,y}$ is a linear through-depth temperature gradient and α the thermal expansion coefficient. If the beam is axially restrained but rotationally free, thermal expansion will cause a uniform compressive stress ($\sigma=E\alpha\Delta T$) across the whole length of the beam where ΔT is the uniform mean temperature rise. This may lead to the beam buckling allowing the increase in length to be accommodated by deflection (although this depends upon the beam slenderness) as in Figure 4. The temperature gradient will cause a uniform axial tension as a result of the thermal curvature trying to pull the beam ends in, as shown in Figure 5.

NUMERICAL ANALYSIS OF A SIMPLE BEAM MODEL

The remainder of this paper describes the results of a geometrically non-linear analysis of a simply-supported universal beam with a slenderness ratio, $l / r = 70$ subjected to heating. The aim of this analysis is to highlight and explain the differences between the behavior and load-carrying mechanisms of an axially restrained and unrestrained beam. The beam has a small through-depth thermal gradient increasing linearly throughout the analysis from 0°C/mm to 0.5°C/mm. It is heated linearly from 0°C to1200°C uniformly, along its entire length. The beam is studied under axially unrestrained conditions and axially restrained conditions typical of the arrangement in a fire resistance test and a multi-story frame structure, respectively. The two models are illustrated in Figure 4. In the British Standard fire resistance test, the beam is allowed to translate laterally as shown in Figure 5(a). Therefore, the increase in length

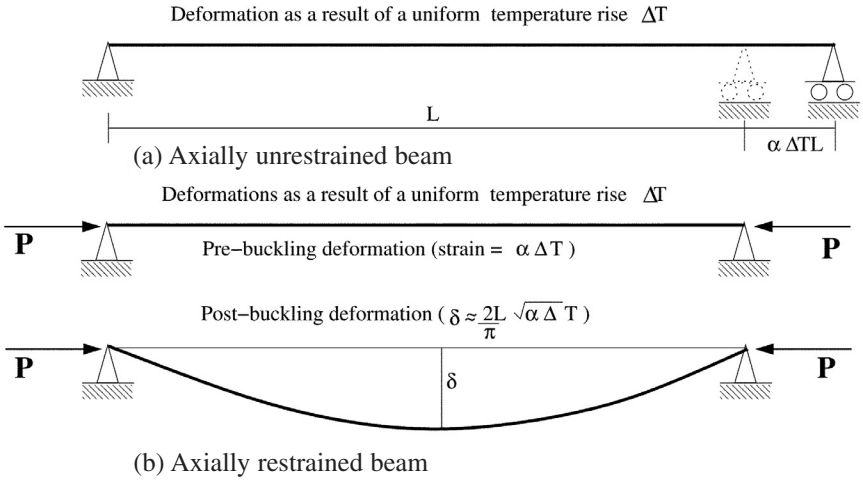

Fig. 4. Thermal expansion of an axially restrained beam.

as a result of thermal expansion is accommodated by simply expanding. Any downward displacement is entirely due to the gravity loading applied. In a real indeterminate structure the beam would experience some degree of restraint against thermal expansion as shown in Figure 5(b), and initially the increase in length would cause strains as the beam is pushed up against the supports. However, if the beam is sufficiently slender, according to Equation 7 the beam will buckle and move into a large displacement nonlinear mode of behavior with no further increase in stress. The temperature at which this may happen is given by Equation 7 (for rigid axial restraint).

$$\Delta T_{cr} = \frac{\pi^2}{\alpha}\left(\frac{r}{l}\right)^2 \tag{7}$$

Figure 6 shows the deflection response of the two beam models. First consider the results of the axially unrestrained beam. Initially there is very little downward deflection because the supports are allowed to translate outwards upon expansion until around 550°C when "runaway" occurs. This happens as a result of the supports being pulled in when the material properties change with increasing temperature and the beam stiffness can no longer support the gravity loading. In stark contrast is the deflection history of the axially-restrained beam. It buckles at around 70°C and as a result has higher initial vertical displacements. "Runaway" is not reached until much later at temperatures around 700°C when the steel stiffness is much reduced. This illustrates that the presence of restraints to end translation delays "runaway" to much higher temperatures because of the development of catenary action to replace the highly depleted flexural stiffness.

The second beam is a better representation of beams in large redundant steel frame structures (structures where horizontal members such as beams and slabs are likely to be restrained against lateral translations). In real composite frame structures, restraint to thermal expansion is available and the steel beam is in composite action with the slab, which produces a much stronger structure. Large deflections seen in real structures are often misinterpreted as impending "runaway" failure. Figure 6 shows that for temperatures below 300°C the deflections for the restrained beam are much higher than for the laterally unrestrained beam but they are not indicative of "runaway." These deflections are caused entirely by the increased length of the beam in a post-buckled state as a result of thermal expansion. In a real structural element in a large structure the large displacements are due to a combination of thermal expansion and thermal bowing effects

The second part of these analyses looks at the effect of loading on the axially-restrained beam. A uniformly distributed load (UDL) w that would achieve the maximum plastic moment M_p (where $M_p = wl^2/8$) at the mid-span of the beam was applied to the model before introducing the heating regime. This process was repeated varying the UDL to obtain a spread of results corresponding to moments lesser and greater than M_p. The results of this analysis are given in Figure 7 where it is shown that the response of the restrained beam with a loading w causing M_p does not achieve "runaway" until 700°C. The beams with UDL causing moments less than M_p, typical of service conditions, do not achieve "runaway" until very high temperatures are reached (typically greater than 800°C). In the early stages of the analysis, before temperatures of 400°C, all the scenarios show similar rates of deflection.

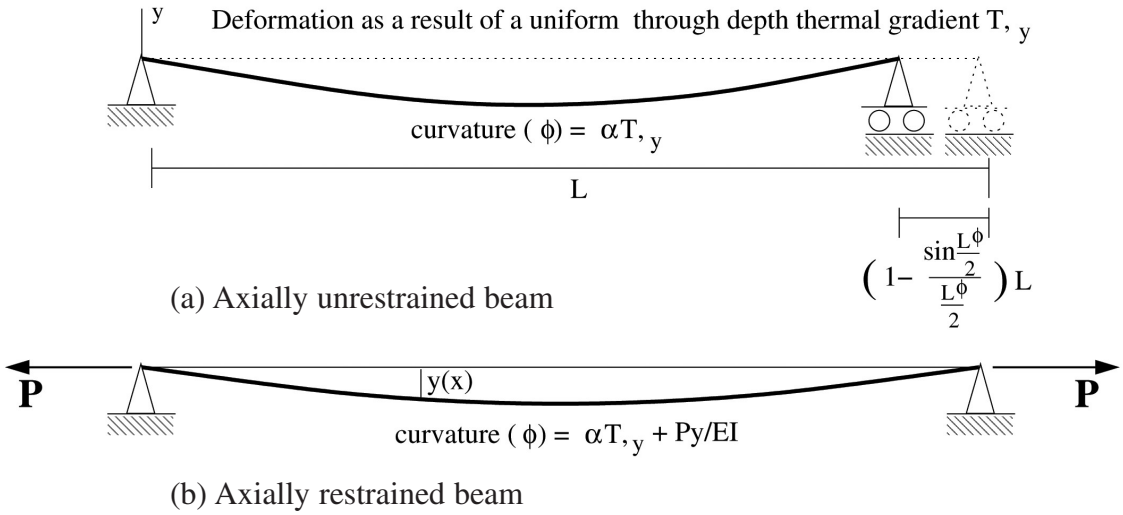

Fig. 5. Thermal bowing of an axially restrained beam.

By differentiating the results plotted in Figure 7 a much clearer picture of runaway failure can be drawn. Figure 8 is a plot of *dy/dT* (rate of deflection change with change in temperature) against increasing temperature, showing the points of "runaway" failure in each load case as a distinct change in gradient.

Deflections before impending structural failure are dominated by thermal effects. The failure temperature is reached when any further deflections are dominated by loading. Initially in Figure 7 the load-deflection curves are parallel to each other for all loads, which indicates that deflections are dominated by temperature rise until a temperature is reached where the beam has weakened to an extent that the loads begin to dominate, leading to "runaway" failure.

As well as looking at the deflection response of the simple beam model to changing loads, the axial forces and moments experienced by the beam were also investigated. For equilibrium to be satisfied at all times the beam must continue to carry the applied moment. Initially flexural resistance of the beam achieves equilibrium with the applied moment. However as the material properties degrade as a result of the increasing temperatures the

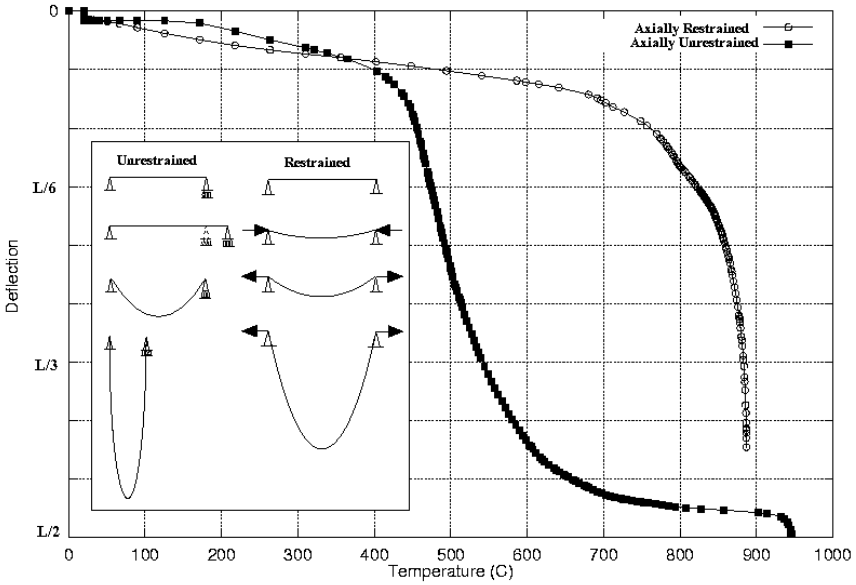

Fig. 6. "Runaway" in a restrained and an unrestrained beam.

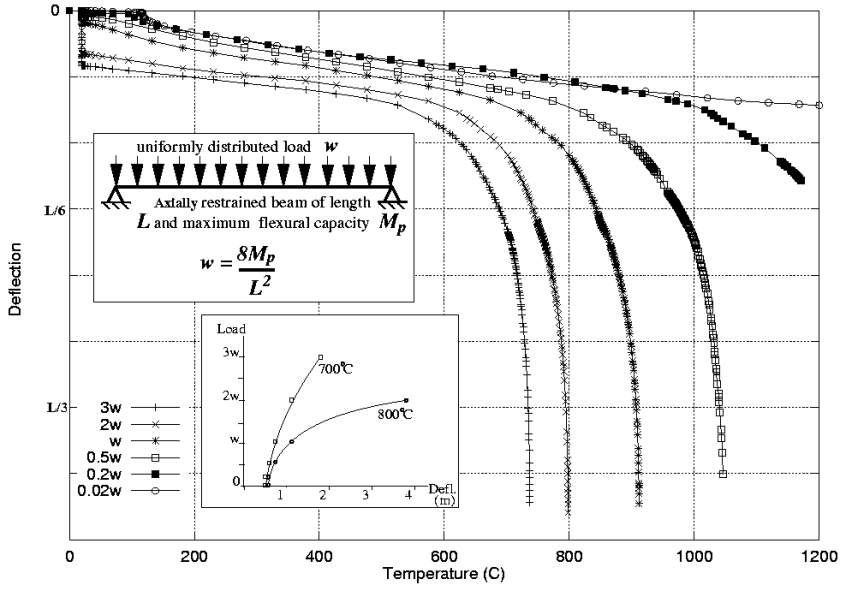

Fig. 7. The effect of loading on a restrained beam subject to heating.

moment capacity of the beam reduces and the applied moment is carried by a combination of the remaining flexural capacity and the P-Δ tensile membrane resistance or catenary action. The equilibrium of the problem is illustrated in Figure 9. The applied moment is $wl^2/8$ and the tensile membrane or catenary resistance is Hd where H is the axial force and d the displacement of the beam at mid-span. Figures 10 through 15 show the bending moments and axial forces generated in the beams for three of the load cases studied (0.5w, 1.0w, 2.0w). In each case, when plotting the moments, the plastic moment capacity of the beam, the P-Δ (tensile membrane resistance), the flexural resistance and the total moment applied to the beam are shown. The plots of axial force show the axial force at the support and at mid-span and the axial (tensile) capacity. These figures highlight the change in load-carrying mechanism as the material properties degrade.

For the load case, 0.5w, the moments and axial forces are plotted in Figure 10 and Figure 11, respectively. In the early stages of the heating regime, up to 400°C, the total moment (from both loading and additional compressive P-Δ moments) is carried by the flexural resistance of the beam. As the moment capacity and the flexural resistance decrease, compressive moments decrease to zero (with increasing deflection), with the entire load being resisted by the residual flexural capacity. Beyond this point the tensile P-Δ moments assist the flexural mechanism in supporting the applied moment. Runaway occurs when both load carrying mechanisms are exhausted. The axial forces consist of a small tension in the beginning, then they increase in compression as the temperature of the beam increases and the beam starts to expand against the rigid supports. After the beam buckles at around 70°C and begins to deflect, the axial force reduces in compression and moves into tension. Towards the end of the analysis, just before impending runaway, the axial tension and the tensile capacity converge.

The explanation is very similar for 1.0w and 2.0w. Figure 12 and Figure 13 illustrate the results of the analysis for a UDL of 1.0w. Initially the plastic moment capacity is equal to the total moment as a result of the load applied. The moment is carried by a combination of flexural resistance and P-Δ tensile membrane resistance from the start. At 20°C there is tensile membrane resistance as a direct result of the gravity loading. The flexural resistance increases up to M_p at 80°C as the tensile membrane resistance drops back to zero. Beyond 100°C the flexure resistance decreases and the tensile membrane resistance increases to maintain equilibrium and carry the applied moment. After 400°C the moment capacity begins to decrease as the material properties of the steel degrade leading to an increased reduction in flexural resistance. Runaway occurs at about 900°C. Figure 13 shows the beam to be in axial tension throughout the analysis because the gravity loading causes catenary action from the very beginning of the analysis. The axial tension decreases a little as thermal expansion causes compression. Above a steel temperature of 500°C the forces increase in tension (to maintain equilibrium by substituting for the declining flexural resistance) and then decrease as the stiffness properties decrease to converge with the tensile capacity of the beam. A UDL of 2.0w results in a total moment equal to double the moment capacity of the beam. Therefore the total moment is carried by a combination of flexural resistance and tensile membrane capacity or catenary action from ambient conditions to the end of the analysis. The high catenary action at ambient is a direct result of the high gravity loading causing large deflections initially (see Figure 7). Once again as the deflections increase as a result of thermal expansion and thermal bowing and the beam loses its stiffness as a result of material degradation the tensile membrane resistance increases and the flexural resistance drops off. Figure 15 shows the high axial tension in the beam at 20°C resulting from the high gravity loading and the decrease in tensile forces as the thermal expansion effects cause compression with increasing temperature. The axial forces and axial capacity converge at "runaway."

IMPLICATIONS

The simple studies discussed in this paper have highlighted the differences in behavior between an unrestrained beam commonly tested in a standard fire resistance test and an axially restrained beam typical of a beam in a highly redundant composite frame structure. It has been shown that "runaway" in an unrestrained beam will occur at much lower temperatures than in the same beam restrained axially. It has also been shown that the load-carrying mechanisms of a restrained beam will change to accommodate the loss of stiffness of the beam as a result of material degradation with temperature. Catenary action develops in the beam as a result of the deflected shape caused by thermal expansion and thermal bowing. Thus the moment applied to the beam is carried by a combination of flexural resistance and tensile membrane resistance. The tensile membrane resistance compensates for the reduction in flexural resistance.

Now that the shortcomings of the fire resistance test have been formally stated. What are the implications? Despite deficiencies it is a universally recognized method of determining the fire resistance of elements of construction.

Present fire resistance gradings of buildings are based on a very simplistic methodology that cannot represent the effects of temperature on a restrained structural element in a highly redundant structure. A thorough scientific understanding of the behavior of the whole structure in fire is needed. Only then can this understanding be incorporated into design codes.

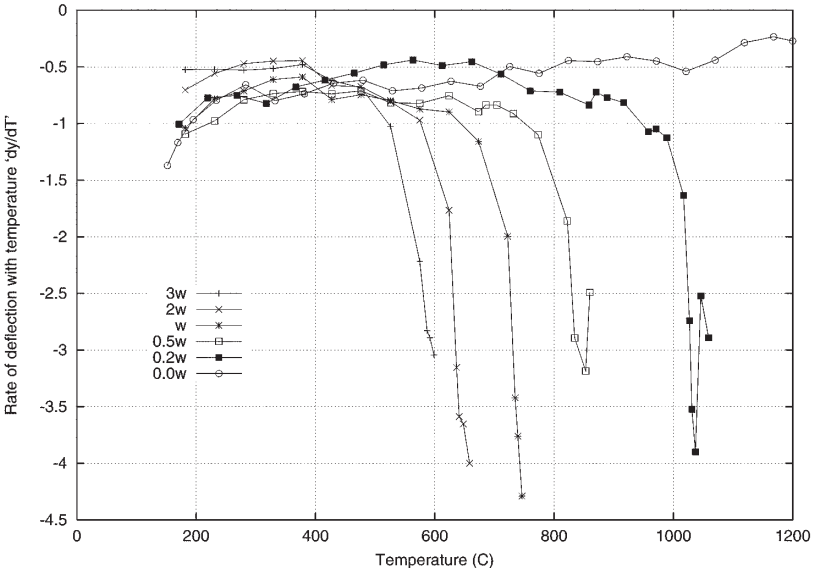

Fig. 8. Loading a heated restrained beam (showing deflection rate of change).

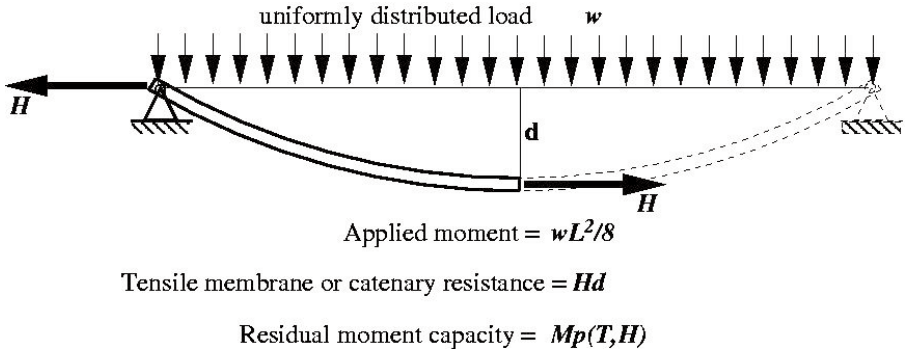

Fig. 9. Catenary action coupled with flexural resistance.

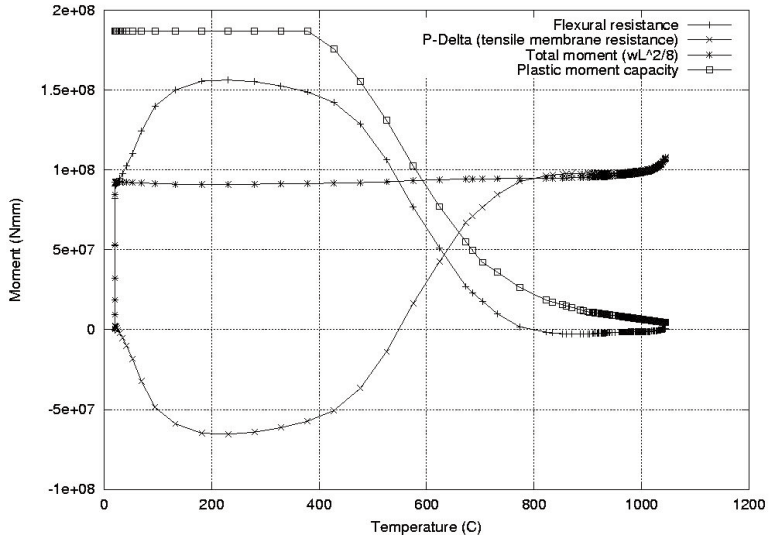

Fig. 10. Moment equilibrium for UDL 0.5w.

Admittedly the above discussion concerns a very simple system and does not consider all the complexity in a real composite frame structure such as the compatibility of deflections in the two directions of a composite floor slab, but nevertheless it highlights the inadequacy of the fire resistance test quite clearly.

CONCLUSIONS

This paper has presented details of the fire resistance test and its context in terms of fire engineering design at present. A review of its history and its shortcomings has been given.

It has been shown that the fire resistance test has little relevance to the behavior of structural elements as part of highly indeterminate structures typical of modern, composite steel frame buildings. The test methods are particularly inadequate when the end conditions during service are unknown and the beam is tested as simply supported, i.e. no consideration of restraint is made. By including the effect of restraint in a simple beam model the temperature at which "runaway" occurs is greatly increased. The reasons

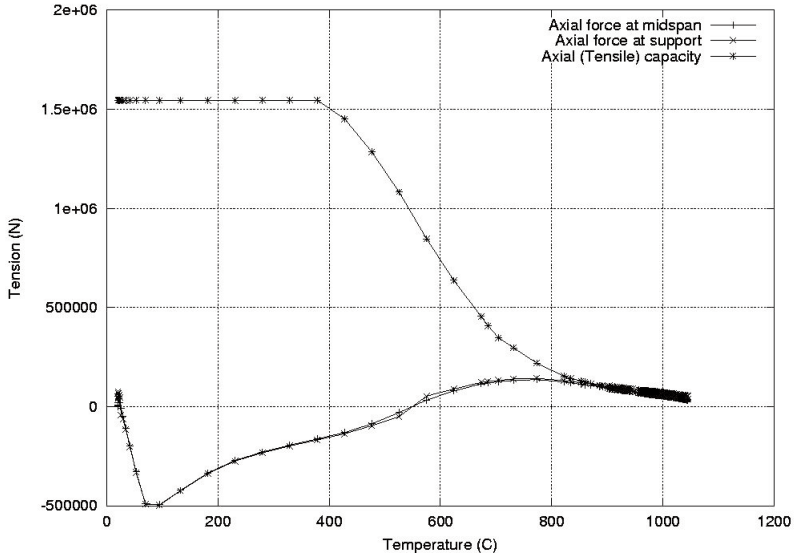

Fig. 11. Axial force for UDL 0.5w.

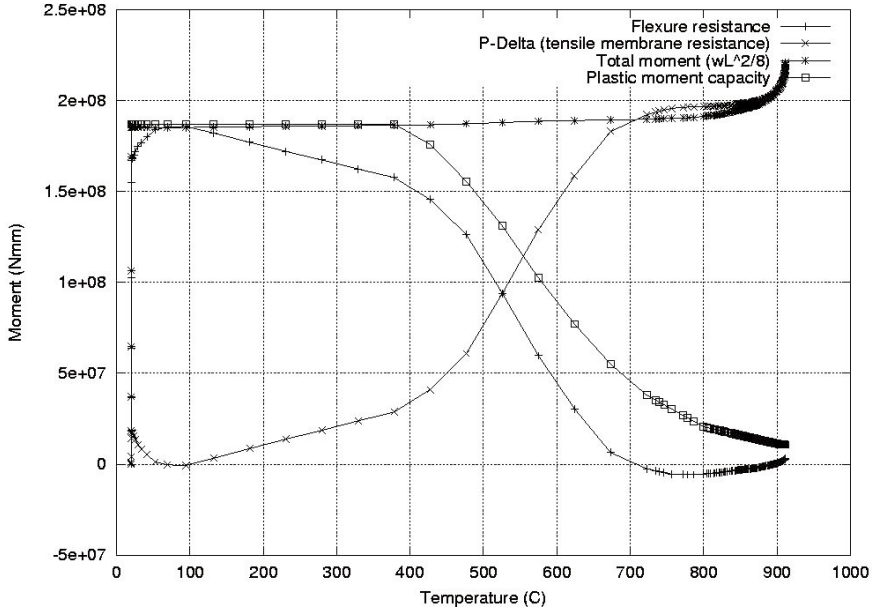

Fig. 12. Moment equilibrium for UDL 1.0w.

for this, i.e. the changing load-carrying mechanisms involved as catenary action develops as a result of the deflected shape have also been explained.

Prescriptive design codes recommend fire gradings for buildings on a simplistic basis. However these simplistic codes were not designed to solve the problems associated with the design of large, modern buildings. The future lies with performance-based design techniques where solutions are tested on an individual basis taking into consideration all aspects of the fire design including the complete structural behavior.

NOMENCLATURE

ϕ	=	thermal curvature
α	=	thermal expansion coefficient
τ_e	=	Equivalent fire resistance, h
ε	=	strain
σ	=	stress, N/mm^2
d	=	deflection, mm
ΔT	=	Change in temperature, °C
A_F	=	Area of floor, m^2
A_t	=	Total area of the compartment boundaries, m^2 [a]

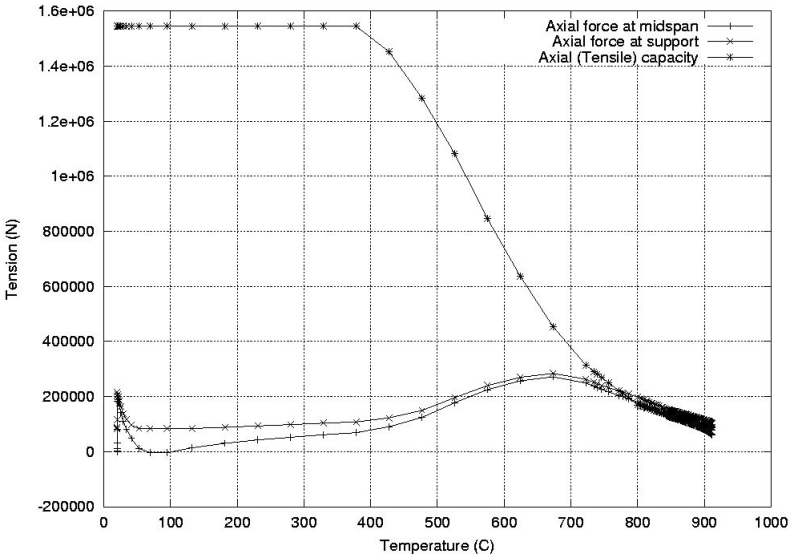

Fig. 13. Axial force for UDL 1.0w.

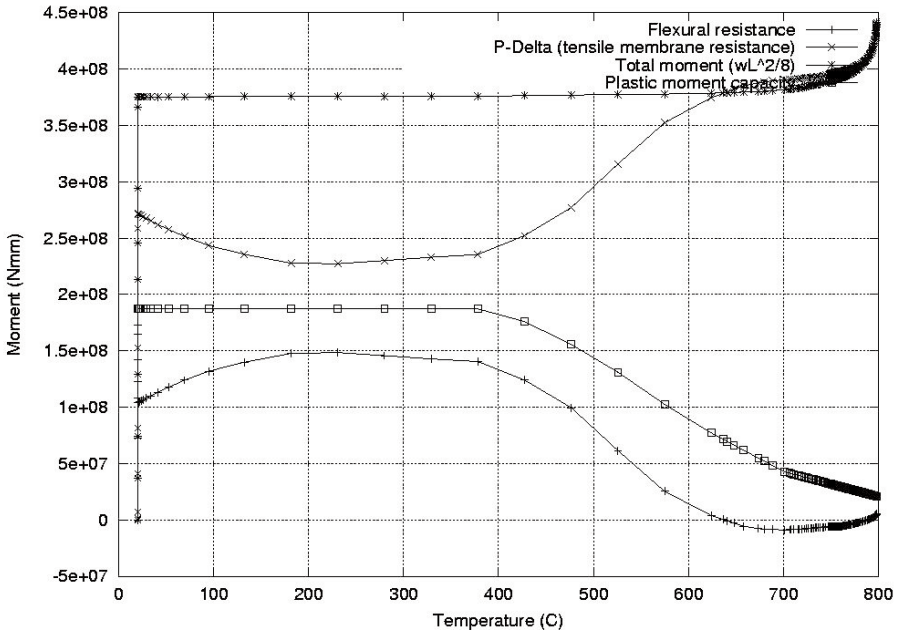

Fig. 14. Moment equilibrium for UDL 2.0w.

[a] Pettersson defines A_t as the area of the boundaries less the area of the openings.

A_v = Area of the ventilation openings, m^2
C = factor depending on the thermal absorptivity of the compartment boundaries, $hm^{3/4}\ kg^{-1}$
E = Young's modulus of elasticity, N/mm^2
H = Horizontal axial force, N
h_v = height of the ventilation opening, mm
l = Clear span of the specimen, mm
L = Fire load, kg/m^2
M = Moment, N-mm
M_c = Moment capacity at 20°C, N-mm
M_f = Applied moment at the fire limit state, N-mm
M_p = Plastic moment capacity, N-mm
P = Point force, N
r = radius of gyration, mm
T = temperature, °C
t = time, sec
$T_{,y}$ = Linear through depth thermal gradient, °C/mm
T_0 = temperature at ambient, °C
w = uniformly distributed load, N/mm

ABBREVIATIONS

ASFP	Association for Specialist Fire Protection
ASTM	American Standard for Testing and Materials
BS	British Standard
DETR	Department of the Environment Transport and Regions
EC	Eurocode
SCI	Steel Construction Institute

REFERENCES

Association for Specialist Fire Protection (ASFP) (2000), "Fire Protection for Structural Steel in Buildings," Steel Construction Institute (SCI) and Fire Test Study Group (FTSG), 2nd Ed., 2nd rev.

ASTM (1995), *Standard Test Methods for Fire Tests of Building Construction and Materials*, ASTM E119-95a, West Conshohocken, Pennsylvania, USA.

Babrauskas, V. and Williamson, R.B. (1978a), "The Historical Basis of Fire Resistance Testing-Part 1," *Fire Technology*, Vol. 14, pp. 185-194.

Babrauskas, V. and Williamson, R.B. (1978b), "The Historical Basis of Fire Resistance Testing-Part 2," *Fire Technology*, Vol. 14, pp. 304-316.

BSI (1987), "Fire Tests on Building Materials and Structures," British Standards Institute, BS476, Part 20-23.

BSI (1990), "Code of Practice for Fire Resistant Design," British Standards Institute, BS5950, Part 8.

Drysdale, D.D. (1998), *An Introduction to Fire Dynamics*, 2nd Ed., John Wiley and Sons, Chichester, UK.

Edinburgh University (2000), "Behavior of Steel Framed Structures under Fire Conditions," DETR(UK) PiT Project Final Report.

Harmathy, T.Z. (1987), "On the Equivalent Fire Exposure," *Fire and Materials*, Vol. 11, pp. 95-104.

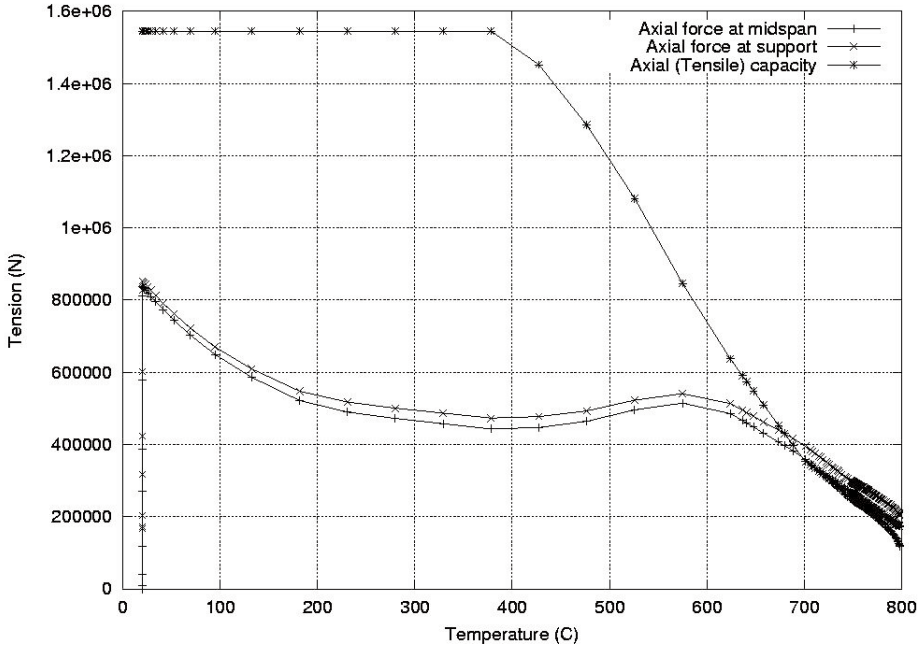

Fig. 15. Axial force for UDL 2.0w.

Ingberg, S.H. (1928), "Fire Loads," *Quarterly Journal of the National Fire Protection Association*, Vol. 22, pp. 43-61.

Law, M. (1971), "A Relationship Between Fire Grading and Building Design and Contents," Fire research note No. 877.

Magnusson, S.E. and Thelanderson, S. (1970), "Temperature-time Curves of Complete Process of Fire Development," ACTA Polytechnica, Scandinavica, *Civil Engineering and Building Construction Series No. 65*, Stockholm.

Malhotra, H.L. (1980), "Fire Resistance Versus Fire Behaviour," Fire Prevention, Vol. 134, pp. 21-27.

Pettersson, O., Magnusson, S.E. and Thor, J. (1976), "Fire Engineering Design of Steel Structures," Swedish Institute of Steel Construction.

The Steel Construction Institute (SCI) (1991), "Structural Fire Engineering Investigation of Broadgate Phase 8 Fire."

Thomas, P.H. and Heselden, A.J.M. (1972), "Fully-developed Fires in Single Compartments. A co-operative research programme of the Conseil Internationale du Batiment," CIB Report No. 20, Fire research note No. 923.

Usmani, A.S., Rotter, J.M., Lamont, S., Sanad, A.M. and Gillie, M. (2001), "Fundamental Principles of Structural Behaviour Under Thermal Effects," *Fire Safety Journal*, Vol. 36, pp. 721-744.